

LOAD FREQUENCY CONTROL IN THREE-AREA SINGLE UNIT POWER SYSTEM CONSIDERING NON-LINEARITIES EFFECT

Narender Saini

Department of Electrical Engineering
National Institute of Technology Kurukshetra
India
narendersaini7379@gmail.com

Jyoti Ohri

Department of Electrical Engineering
National Institute of Technology Kurukshetra
India
ohrijyoti@nitkkr.ac.in

Article history:

Received 13.11.2022, Accepted 25.05.2023

Abstract

Load frequency control is always a crucial aspect in delivering quality power in integrated power system. This paper proposes an optimally tuned Proportional-Integral-Derivative (PID) controller to remove frequency errors caused by unexpected load fluctuations while ensuring tie-line power exchange. Moreover, the three-area power system with non-linearities such as Generation Rate Constraint and Governor Dead Band has been investigated. For tuning the parameters of PID controller Improved Grey Wolf Optimization (IGWO) has been used. The dynamic response of optimized PID controller have been compared with the result obtained from Genetic Algorithm (GA), Particle Swarm Optimization (PSO), and Sine Cosine Algorithm (SCA).

Key words

Load Frequency Control, PID controller, generation rate constraint, Frequency deviation, Improved Grey Wolf Optimization.

1 Introduction

Controlling a power system is one of the most difficult tasks in control engineering. Transmission of electricity having so much fluctuation due to variation of generation, transmission lines, protection devices and control loops etc. The variations in load primarily impact the frequency of the power system network. One of the most important operations for excellent power system management is load frequency control (LFC). The basic goal of LFC is to maintain zero frequency variations by employing controllers to ensure appropriate symmetry between the power required and the power generated. The two types of frequency controllers are classified as:

1. Primary frequency control: - Operating time limits

of primary frequency control is 2 to 20 sec. It may be divided majorly into two categories.

- The Inertial response, also known as the quick response. System's inertia determines how quickly the frequency responds to changes in load or generation, while the control mechanism adjusts the generation output to maintain a stable frequency.
- Governor response, called as a sluggish response.

2. Secondary/supplementary frequency control: - This is usually known as AGC or LFC. Its operating time is 20 sec. to 2 min. Whenever imbalance occur between the load demand and generated power, it helps in maintaining the system's frequency and regulates the power exchange between the interconnected area.

Primary frequency control: — Operating time limits of primary frequency control is 2 to 20 sec. It may be divided majorly into two categories. The Inertial response, also known as the quick response. System's inertia determines how quickly the frequency responds to changes in load or generation, while the control mechanism adjusts the generation output to maintain a stable frequency. Governor response, called as a sluggish response. Secondary/supplementary frequency control: - This is usually known as AGC or LFC. Its operating time is 20 sec. to 2 min. Whenever imbalance occur between the load demand and generated power, it helps in maintaining the system's frequency and regulates the power exchange between the interconnected area.

Various types of controller and techniques are designed throughout the last years for the LFC issue. For the AGC of the multi-area power system, the idea of advanced optimum control was initially presented in [Elgerd and Fosha, 1970]. The load frequency control

problem for single area thermal power systems [Ismayil et al., 2014], single area multi-unit systems [Padhan and Majhi, 2013], and single area hydro-power system is presented in [Arya, 2018]. In the paper [Saini and Ohri, 2022], the LFC for a multi-area power system is provided. Frequency control for the two area single source interconnected system is introduced in [Sahu et al., 2016b; Gupta et al., 2013]. In [Sharma and Saikia, 2015] the LFC of three area with reheat turbine and GRC effect is presented. Controller to reduce the frequency error and maintain the power exchanged in multi-area multiunit system is presented in [Morsali et al., 2017]. The Pchelkina and Fradkov algorithm is modified to make the control system design in [Furtat et al., 2016]. PID as a supplementary controller is suggested for a five-area reheated thermal power plant in [Jagatheesan et al., 2017]. Various kind of controllers such as Fuzzy classical controller [Arya, 2018], PI controller [Guha et al., 2018; Fathy and Kassem, 2019], PID controller [Saini and Ohri, 2023], Type II fuzzy PID [Sahu et al., 2018], Fractional order PID [Abdelmoumene et al., 2018], Model Predictive Control (MPC) [Ismail and Bendary, 2018; Yang et al., 2019], Sliding mode control [Guo, 2019; Lai et al., 2021] is commonly used in the AGC as a secondary/supplementary control to keep the frequency stable.

Most of the researchers used conventional controllers for the LFC and it was observed that the controller's performance totally depends upon the selection of value of the controller parameters. So, the main task is to determine the optimal value of the controller's gain for the enhancement of their performance. In the past, classical approaches such as ZN etc., are used to tune the controller which are totally hit and trial methods. Because the power system has many non-linearities and load demand varies continuously, and these methods do not meet up the requirement. Therefore, we need some advanced methods which can work efficiently. To cop up with these difficulties heuristic and meta-heuristic approaches such as Particle Swarm Optimization (PSO) [Dhillon et al., 2015], Teaching Learning Based Optimization (TLBO) [Sahu et al., 2016a], Genetic Algorithm (GA), Bat algorithm (BA) [Dash et al., 2015], Backtracking Search Optimization Algorithm (BSA) [Jagatheesan et al., 2017], Ant-Lion Optimizer (ALO) [Saikia and Sinha, 2016], Salp Swarm Optimization (SSO), Differential Evolution (DE), Imperialist Competitive Algorithm (ICA) [Elsisi et al., 2015], Firefly Algorithm (FA) [Jagatheesan et al., 2017], Artificial Bee Colony (ABC) [Naidu et al., 2014], and Bacterial Foraging Optimization Algorithm (BFOA) [Ali and Abd-Elazim, 2013] Optimization, Grey Wolf Optimization (GWO) [Saini and Ohri, 2023], Ziegler-Nichols etc. are come into consideration. These approaches are commonly employed by investigators due to their simplicity and avoidance of local optima.

Unfortunately, the majority of the optimization techniques suffer from premature convergence, parametric

sensitivity, and complicated computing. Frequently employed PSO and GA algorithm in LFC, may get stuck in local minima. In the DE algorithm, the control parameters that influence performance are the crossover rate and scale factor. FA [Jagatheesan et al., 2017] is under the control of three different factors (α , β , and γ). When it comes to the effectiveness of the algorithms, the choice of these parameters is of the utmost importance. In order to solve these limitations, the improved grey wolf optimizer (I-GWO) is implemented in this study. The Improved GWO algorithm, does not call for any regulating parameters. This is the motivation to utilize I-GWO method in this study to optimize PID controller parameters because of its simplicity, effectiveness, and speed due to the absence of any parameters required by the algorithm. A number of optimization strategies are employed to calculate the optimum gain values of PID controller in literature. In the present work, using the IGWO along with GA, PSO, SCA method, the controller's ability is evaluated to manage frequency fluctuations in the considered power systems. According to the simulation findings, the IGWO-optimized PID controller surpasses the other optimization techniques in every manner. Finally, the stability of the IGWO based PID is investigated in the presence of uncertainties, by modifying the system's characteristics, such as the turbine and governor time constants, both by up to 25%. The contribution of the paper lies in the following aspects:

1. Development of a Improved Grey Wolf Optimized PID controller to regulate the system's frequency in a three-area power system.
2. Evaluation of the effectiveness of the PID controller in the presence of various uncertainties such as load disturbances, system non-linearities such as GRC and GDB, and parameter variations.
3. Comparison of the performance of the IGWO based PID controller with other controllers such as SCA/PSO/GA based PID controllers.
4. Analysis of the robustness of the IGWO based PID controller under different operating conditions and uncertainties.
5. Validation of the PID controller using simulation studies in MATLAB/Simulink.

The rest of the paper is as follows; Section 2 represents the test system and controller's modeling. Section 3 provides a quick overview of the IGWO algorithm and other approaches. Simulation results obtained by IGWO and other considered techniques are provided in the section 4, Lastly, section 5 conclude the paper.

2 Power system model

In this work, a three-area single unit power system model is considered as shown in figure1 [Sahu et al., 2016a]. The rating of each unit in each area is 2 GW, 4

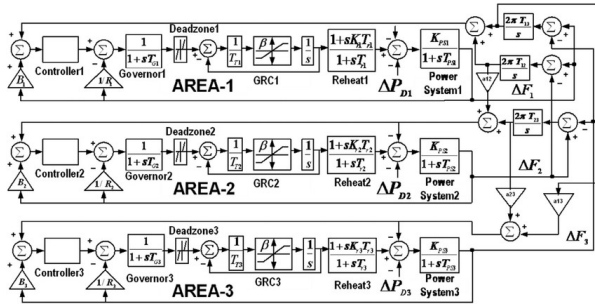


Figure 1: Three unequal area -power system model

Table 1: System's parameters values

$R_1 = 3.0$	$R_2 = 2.73$	$R_3 = 2.82$
$K_{p1} = 66.6$	$K_{p2} = 62.5$	$K_{p3} = 66.6$
$B_1 = 0.348$	$B_2 = 0.382$	$B_3 = 0.369$
$T_{g1} = 0.08$	$T_{g2} = 0.06$	$T_{g3} = 0.07$
$T_{t1} = 0.4$	$T_{t2} = 0.44$	$T_{t3} = 0.3$
$T_{P1} = 0.185$	$T_{P2} = 0.21$	$T_{P3} = 0.138$
$K_{r1} = 0.5$	$K_{r2} = 0.5$	$K_{r3} = 0.5$
$T_{r1} = 10$	$T_{r2} = 10$	$T_{r3} = 10$

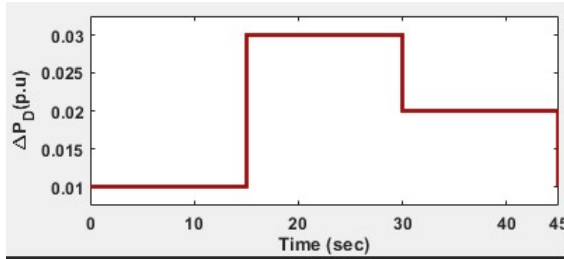


Figure 2: Random change in power demand

GW and 8 GW. In most of articles, physical constraints are not considered. Taking into consideration all the physical constraints may be a difficult task and not useful too but some constraints, such as Generation Rate Constraints (GRC) and Governor Dead Band (GDB) must be considered to analyze the system's performance perfectly. If these constraints are not considered then the frequency and tie-line power variations could be nullified in a concise period, the considered system can also chase large disturbances in the load. But when these constraints are considered, system becomes non-linear and more deviations occur in the area control error. In the thermal power station, power cannot be generated immediately. It can generate power at a specified rate only (3-5%/min.), called GRC. So, in this work, the effect of GRC is also considered to match the tested system with the practical scenario. The shift in speed within which the governor valve position remains unchanged is called as governor dead band action. The GDB has a significant impact on the electrical power system's performance. In the system, it tends to create a sustained sinusoidal oscillation. The present work considered the backlash non-

linearity of 0.05% ie. 0.03 (0.025 in case frequency is considered as 50 Hz). When GRC is used in combination with the GDB, the negative effect of GRC is amplified, and the system's frequency may not achieve its nominal value within a certain time period. The transfer function of each unit consists of governor, turbine and reheat turbine are used in the model for simulation process. A governor transfer function is given by

$$G(s) = \frac{1}{1 + sT_g} \quad (1)$$

Turbine's transfer function [Wood et al., 2013] is

$$T(s) = \frac{1}{1 + sT_t} \quad (2)$$

Thermal power plants often use reheat turbines as well, and its transfer function is given by

$$T_R(s) = \frac{1 + sK_r T_r}{1 + sT_r} \quad (3)$$

The overall transfer function [Wood et al., 2013] of the load and generator is

$$P(s) = \frac{K_p}{1 + sT_P} \quad (4)$$

The parameters values of the power system model used in the simulation process are given in Table1 as:

2.1 Random change in load demand

Usually, the researchers considered the step change in load demand, but in this work, along with step change, a random load change has been considered. The variation that occurs in simulation is shown in the figure2 below.

2.2 Controller and objective

Since there is an arbitrary change in the power demand due to which frequency deviates from its nominal value so as to sustain inter-tie power exchange between related areas and manage frequency deviations, a controller is required so in this work, PID controller is employed in each area to solve the aforementioned issue. It is the most commonly used controller by researchers. It helps in improving the system performance by minimizing the peak undershoot and overshoot in the response within significantly less time. The transfer function for the PID controller is

$$T_{PID} = K_P + \frac{K_I}{S} + K_D \quad (5)$$

The PID controller functioning depends on gains value, so selection of optimal values of gain is of utmost importance. In this work GA, PSO, SCA, and IGWO techniques are employed to accomplish this task. Whenever

any unexpected load changes occur, the needed ACE in each area triggers the controller movement. The ACE signal is comprised of the incremental tie-line power and frequency change, and is given by

$$ACE_1 = B_1 \Delta f_1 + P_{tie1} \quad (6)$$

$$ACE_2 = B_2 \Delta f_2 + P_{tie2} \quad (7)$$

$$ACE_3 = B_3 \Delta f_3 + P_{tie3} \quad (8)$$

Where Δf_1 , Δf_2 and Δf_3 are change in system's frequency and P_{tie1} , P_{tie2} and P_{tie3} are the power flow through the tie-lines. In the frequency control, for the better functioning of the controller or system the performance index (P.I) value should be minimum. Performance index value decide controller's performance. Generally, four types of P.I are used, and ITAE is one of them and is chosen in this work. The ITAE expression is mainly composed of the frequency and the tie-line power change, as shown below.

$$P.I = ITAE = \int_0^{t_s} \sum_{p=1}^3 (|\Delta f_p| + |\Delta P_{tie-p}|) dt \quad (9)$$

3 Optimization techniques

This work proposes the IGWO technique to minimize the performance index given in (9) and optimize the controller performance for frequency control and sustain tie line power exchange despite physical limits in the thermal power system such as GRC and GDB. The brief description about the IGWO is given below. Optimization techniques SCA, PSO, GA [Mirjalili, 2016; Alam, 2016] are also employed in this work for the comparison purpose.

3.1 Improved Grey wolf optimization (IGWO)

Mirjalili et al. developed GWO in 2014, a meta-heuristic method based on grey wolves' natural leadership and hunting behaviour. In the nature, they are thought to be apex predators and live in groups (packs). In a typical group, there are 8-14 members. Every member in the group has its significance. Alpha (α), Beta (β), Delta (δ) and Omega (Ω) are the four levels of wolves in their group. Tracking the target, chasing and approaching it, surrounding and tormenting it until the prey comes to a complete stop, and then attacking the target are all part of the hunting process. The target's location is suggested by α , β , and δ , and then the remaining wolves, i.e., omega, in search of the fittest search agent they, renovate their place.

Although the GWO is beneficial, it is insufficient to produce a feasible solution. So some improvement is done in the GWO by Mohammad H. et al. in 2020 [32]. The I-GWO develops its movement strategy by incorporating the dimension learning-based hunting (DLH)

search method inspired by the individual hunting of wolves. Finally, depending on the quality of their new placements, the I-GWO's strategy chooses a candidate from either the GWO or DLH search methods. The collaboration between these two search techniques increases the proposed algorithm's global and local search capabilities.

3.2 Mathematical model of Grey wolf optimization

The fittest solution is alpha, followed by beta, and finally delta in the GWO. Omega is the name for the rest of them. α , β , and δ generally direct the hunting process in the GWO algorithm and ω have to be followed these three wolves. Following are the mathematical equations for encircling behavior:

$$D = |CP_p(t) - P(t)| \quad (10)$$

$$P(t+1) = P_p(t) - A.D \quad (11)$$

where,

t is the current iteration

The following are the vectors A and C

$$A = 2a.r_1 - a \quad (12)$$

$$C = 2.r_2 \quad (13)$$

where,

Over the course of repetitions, the components of a are progressively lowered from 2 to 0.

r_1 and r_2 are the random vectors in [0, 1].

Occasionally, the β , and δ wolves participate in the hunting operation. As a consequence, α , β , and δ will have a better idea of where the prey is. The top three solutions α , β , and δ have been saved, and the remaining agents must renovate their locations to resemble the best search agents' place.

$$D_\alpha = |C_1.P_\alpha - P(t)| \quad (14)$$

$$P_1 = P_\alpha - A_1 D_\alpha \quad (15)$$

$$D_\beta = |C_2.P_\beta - P(t)| \quad (16)$$

$$P_2 = P_\beta - A_2 D_\beta \quad (17)$$

$$D_\delta = |C_3.P_\delta - P(t)| \quad (18)$$

Table 2: Controller parameters for different optimization

	Area-1			Area-2			Area-3		
	K_P	K_I	K_D	K_P	K_I	K_D	K_P	K_I	K_D
GA	1.7369	0.0883	0.4769	1.6169	0.3222	1.7012	0.7498	0.2245	0.9793
PSO	2.0	0.0693	0.9153	2.0	0.0842	2.0	0.1529	0.0809	0.0000011
SCA	-0.12789	0.07237	0.15136	0.6121	0.076502	-0.089171	0.52581	0.0037864	0.23846
IGWO	4.5091	0.1113	2.5764	11.9889	0.1527	0.5378	4.3431	0.1513	0.8290

$$P_3 = P_\delta - A_3 D_\delta \quad (19)$$

$$P(t+1) = \frac{P_1 + P_2 + P_3}{3} \quad (20)$$

When the target's movement comes to a halt, the grey wolves attack it. Although the GWO is beneficial, it is insufficient to produce a feasible solution. So some improvement is done in the GWO by Mohammad H. et al. in 2020 [Nadimi-Shahraki et al., 2021]. In next section, an Improved Grey Wolf Optimizer (I-GWO) includes a new search method connected with a stage of selecting and updating in order to overcome these concerns.

3.3 Mathematical Model of Improved Grey Wolf Optimization

The I-GWO consists of three phases: initializing, moving, and choosing and updating.

3.3.1 Initialization phase: During this phase, M wolves are placed randomly across a specific range $[l_j, u_j]$ in the search space.

$$P_{ij} = l_j + rand_j[0, 1] \times (u_j - l_j); i \in [1, M]; j \in [1, Dim] \quad (21)$$

At the t^{th} iteration, the position of the i^{th} wolf is represented as a vector of real values called $P_i(t) = [P_{i1}, P_{i2}, \dots, P_{iDim}]$, where Dim is the number of dimensions in the issue. This vector is then iterated until the problem is solved. A matrix called Pop that has M rows and Dim columns stores information on the whole wolf population. The fitness function, denoted by $f(P_i(t))$, is responsible for computing the value of $P_i(t)$ fitness.

3.3.2 Movement phase: According to the information provided above section, in classical GWO approach, the α , β , and δ refer to the first three finest wolves that come from Pop. Following that, the equations 12-13 are used to derive the coefficients A and C . After that, one determines the prey surrounding by considering the locations of P_α , P_β , and P_δ using the equations 14 to 20. In conclusion, the equation used to determine the first contender for the new location of wolf $P_i(t)$ is shown by equation 20.

In the classical GWO, each wolf is assigned a new place with the assistance of three leading wolves of the Pop. This causes GWO to converge slowly, and wolves to get locked in the local optimum. Individuals hunting are included in the proposed DLH search approach to tackle these issues. Each dimension of the new location in DLH search of $P_i(t)$ is determined by Eq. 23 in which this particular wolf is learned by its diverse neighbors and a randomly picked wolf from Pop. Calculating $R_i(t)$ involves finding the Euclidean distance between the present location of $P_i(t)$ and the candidate position $P_{i-GWO}(t+1)$, which is done with the help of the equation 22.

$$R_i(t) = \|P_i(t) - P_{i-GWO}(t+1)\| \quad (22)$$

The equation 23 determines the neighbors of $P_i(t)$, represented by $M_i(t)$, with regard to the radius $R_i(t)$, where Dim_i is the Euclidean distance between $P_i(t)$ and $P_j(t)$.

$$M_i(t) = P_j(t) | Dim_i(P_i(t), P_j(t)) \leq R_i(t), P_j(t) \in Pop \quad (23)$$

After the neighborhood of $P_i(t)$ is created, Equation 24 does multi-neighborhood learning

$$P_{i-DLH,d}(t+1) = P_{i,d}(t) + rand \times P_{n,d}(t) - P_{r,d}(t) \quad (24)$$

3.3.3 Phase of Choosing and Updating Candidates: In this phase, initially, the superior candidate is picked by comparing the fitness values of two candidates named $P_{i-GWO}(t+1)$ and $P_{i-DLH}(t+1)$ using the equation 25.

$$N_i(t) = P_j(t) | D_i(P_i(t), P_j(t)) \leq R_i(t), P_j(t) \in Pop \quad (25)$$

If the chosen candidate has a lower fitness value than $P_i(t)$, then $P_i(t)$ is modified to reflect the new position of $P_i(t+1)$. If nothing else changes, $P_i(t)$ in the Pop will stay the same. When this process has been repeated for every single individual, the iteration counter is incremented by one and the search is repeated until a maximum number of iterations has been achieved.

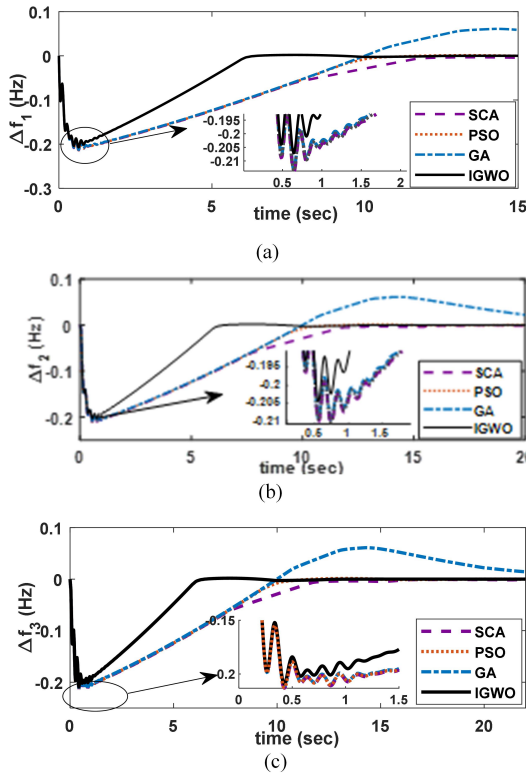


Figure 4: Frequency change (a) Δf_1 in area-1 (b) Δf_2 in area-2 and (c) Δf_3 in area-3

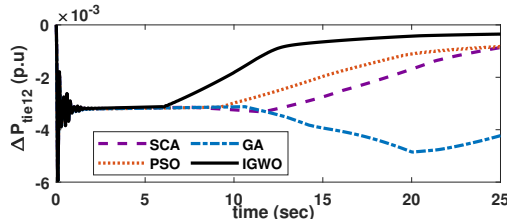


Figure 5:

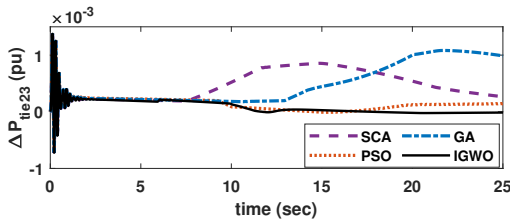


Figure 6:

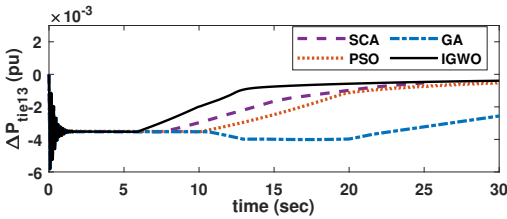


Figure 7:

Figure 8: Tie line power variation (a) ΔP_{tie12} within area-1 and area-2 (b) ΔP_{tie23} within area-2 and area-3 and (c) ΔP_{tie13} within area-1 and area-3

3.4 Simulation experiment and results

Model of a three-area power system with a non-reheat turbine, GRC and GDB undertaken for this study is

shown in Fig.1. Two types of load changes are considered one is step load change (0.01 p.u) and second is randomly load change shown in Fig.2. Two controllers employed in each area is of PID type. The considered model is designed using the MATLAB (Simulink) platform.

3.4.1 System response with 1% (0.01 p.u) step load change in area-1:

In this case a step load change of 1% (0.01 p.u) in area-1 is considered. The ITAE is considered as objective in the optimization process. Since the GRC is an important factor in LFC so it is considered in this model and its value is taken as 0.0005 MW p.u/sec i.e. 3%/min. Both the population size and iterations are taken as 30. Each area has its own PID controller, and its parameters are optimized using the GA, PSO, SCA, and IGWO algorithms. The obtained ultimate optimum gain values of PID controller by using considered optimization techniques are given in the Table 2.

The convergence of the cost curve (ITAE) w.r.t the no. of iterations of different optimization techniques is shown in Figure3. The following figure demonstrates that IGWO converges to minimum value in a very short range as compared to other techniques.

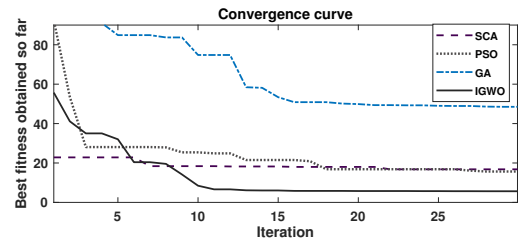


Figure 3: Convergence curve of different optimization techniques

The frequency deviation in all the three areas and tie-line power change obtained from the simulation experiment using GWO optimized PID controller and other considered optimization-based controllers are shown in Fig. 4 to 5. The table 3 provides the settling time (in seconds) for various control techniques for different control variables, namely Δf_1 , Δf_2 , Δf_3 , ΔP_{tie12} , ΔP_{tie23} , and ΔP_{tie13} , based on the ITAE performance index.

It is observed from Table 3 and the above figures that the settling time for frequency change in area-1 (Δf_1) for IGWO is 6.0879, which is 76.52% lower than GA. Similarly, the percentage reductions for PSO and SCA are 41.04% and 69.27%, respectively. Similarly, the settling time for the change in power flow through tie-lines between area-1 and area-2 (ΔP_{tie12}), the settling time with IGWO is 71.29% better than GA, 62.21% better than PSO, and 58.36% better than SCA.

So, Overall, the above figures and table clearly demonstrate that IGWO is the best optimization technique among GA, PSO, and SCA in terms of settling time for a three-area power system. It achieves faster settling times by a large margin, as evidenced by the percentage im-

Table 3: GWO performance compared based on error, overshoot value and settling time

Technique	Settling time (sec) for						ITAE
	Δf_1	Δf_2	Δf_3	ΔP_{tie12}	ΔP_{tie23}	ΔP_{tie13}	
GA	25.913	25.858	25.872	53.17	52.296	52.382	48.51
PSO	10.326	10.328	10.305	40.621	38.3	39.644	15.672
SCA	19.812	20.191	19.697	36.937	35.643	36.23	16.7872
IGWO	6.0879	6.1165	6.0951	15.259	23.256	15.658	5.651

improvements over the other techniques. These results indicate that IGWO can be a valuable tool for improving the performance of power systems. For a better understanding, the graphical depiction of performance indices is presented in the form of a bar chart and can be seen in Figure 11.

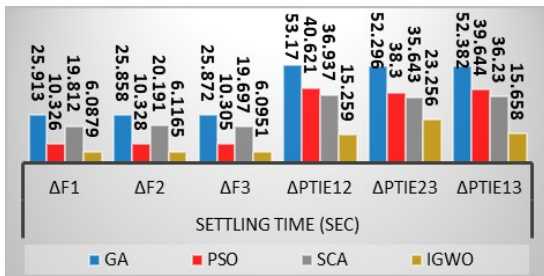


Figure 9:



Figure 10:

Figure 11: Comparison of GWO-based PID controller with other techniques for three area control

3.5 System performance with random change in load

This simulation experiment is performed for the frequency control of a three-area single source system with random load changes depicted in Fig. 2 in area-1 using the IGWO optimization approach. As it has been observed from the simulation experiment presented in section 4.1 that IGWO gives the more superior performance and convergence then the other optimization techniques considered in this work. Hence the results obtained with IGWO, are only shown in this section.

The system response obtained for change in frequency (Δf_1 , Δf_2 and Δf_3) in all three areas and the power flow through the tie-line between (ΔP_{tie}) are shown in Fig. 7 and fig.8 respectively. Since the change in load is unexpected, it can occur anytime so to check the effectiveness of proposed approaches random change in load is considered in area-1. The figures below demonstrate this clearly that IGWO optimized PID controller

has efficiently handled the random change in load demand and nullified the frequency error in very less time, and maintained the tie-line power exchange. IGWO optimized PID controller response gives the reduced under-shoot value and the oscillations in the response.

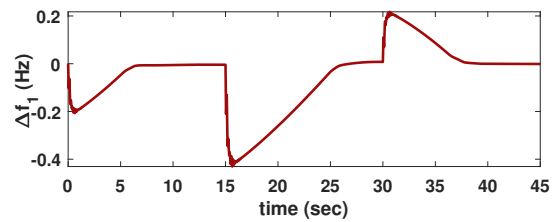


Figure 12:

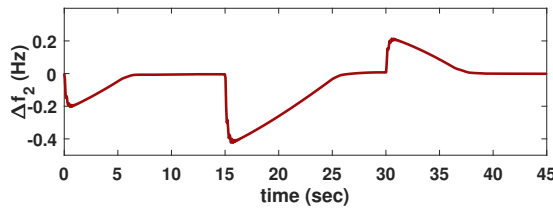


Figure 13:

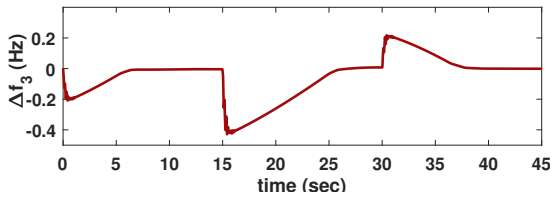


Figure 14:

Figure 15: Frequency variations (a) in area-1 (Δf_1), (b) in area-2 (Δf_2), and (c) in area-3 (Δf_3) with random load change

It is clearly seen from the fig. 8 to 9 that IGWO based PID controller is able to eliminate the fluctuation in the frequency of both areas and oscillations in the tie-line power in very little time which occurs due to the power demand changes with respect to time.

3.6 Sensitivity Analysis

A simulation experiment is performed to verify the robustness of the selected control mechanisms, hence sensitivity analysis is conducted by modifying the system's parameters. Three cases of the parameter's uncertainties have been considered as

1. Case-1: - change in turbine time constant (T_T) up to $\pm 25\%$.

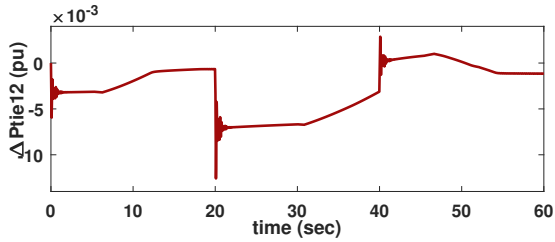


Figure 16:

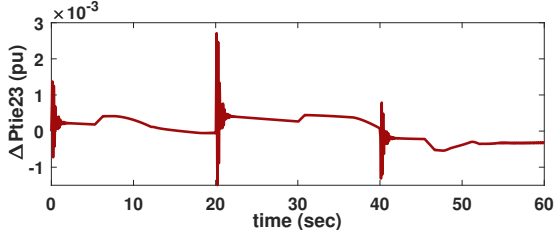


Figure 17:

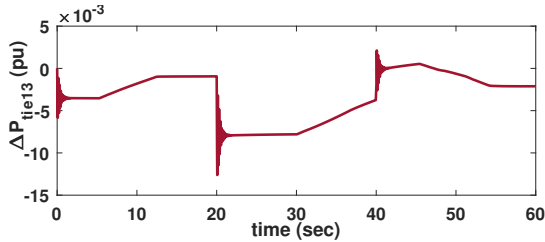


Figure 18:

Figure 19: Tie line power variation (a) within area-1 and area-2 (ΔP_{tie12}), (b) within area-2 and area-3 (ΔP_{tie23}) and (c) within area-1 and area-3 (ΔP_{tie13}) with random load change

2. Case-2: - change in governor time constant (T_G) up to $\pm 25\%$.
3. Case-3: - The change in turbine and governor time constant up to $\pm 25\%$ are applied simultaneously.

Under nominal conditions, the PID gains value obtained from the IGWO optimization approach is preserved. As a result of the aforementioned scenarios, the system's parameters are changed to introduced the uncertainties. The PID gains value derived from the nominal condition are selected in this sensitivity analysis process for all the three cases of uncertainties. The frequency changes (Δf_1 , Δf_2 and Δf_3) in all the three areas and tie-line power change between them (ΔP_{tie12} , ΔP_{tie13} , and ΔP_{tie23}) for the above cases are shown in Fig.9 to 11. Above figures shows the robustness of the IGWO optimized PID controller as it is clearly seen that the IGWO is very efficient in controlling the frequency and the tie-line power deviations whenever changes occur in the system's parameters values and for large changes in the system's parameters, the optimal value of the controller's gains determined at the nominal condition with nominal parameters does not need to be reset.

4 Conclusion

The goal of LFC is to stabilize the tie-line power and frequency oscillations in the system. With the rising de-

mand for electricity, it's more important than ever to have a robust LFC system that can handle system parameter uncertainty. GA, PSO, SCA, and IGWO optimization techniques have been employed in this work to find the optimal values for the PID controller's gains for the LFC of multi-area power system. A three-area single unit with GRC and GDB effect is considered in this work. Step load change of 1% (0.01 pu) and dynamic load change has been considered in area-1. Better performance of IGWO based PID controller is observed in LFC as compared to GA, PSO and SCA based PID controller in terms of minimization of performance indices for the considered system. In addition to it, the robustness of the controller is also ascertained in presence of uncertainties in system's parameters such as turbine and governor time constant individually and both simultaneously in the range of $\pm 25\%$ for both the systems. The simulation results reveal that the performance under the parameter's uncertainties and normal conditions are more or less the same, the settling time value for the frequency error and tie-line power change vary within an acceptable range. Thus, the IGWO optimized PID parameters obtained at nominal values are robust and stable.

References

Abdelmoumene, D., Salem, A., and Lakhdar, M. (2018). Load frequency control problem in interconnected

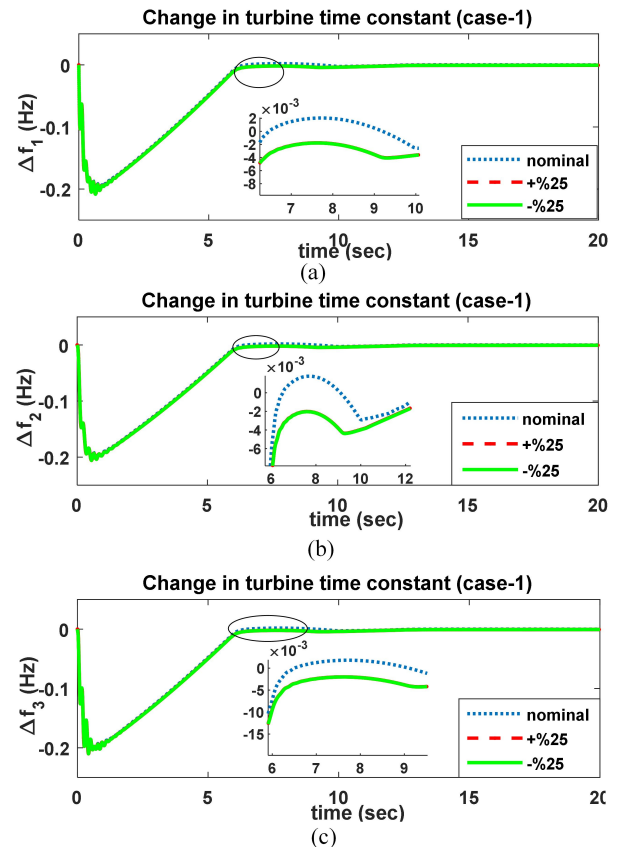


Figure 20: Response of three area system for case-1

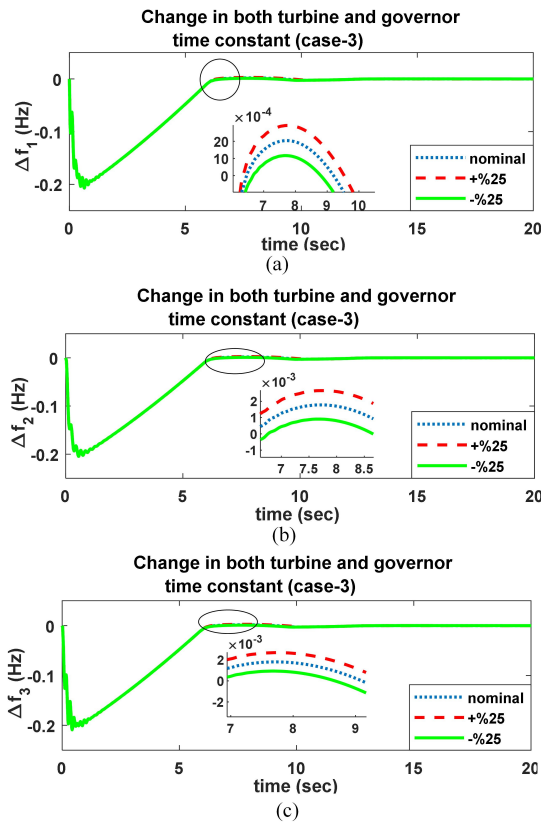
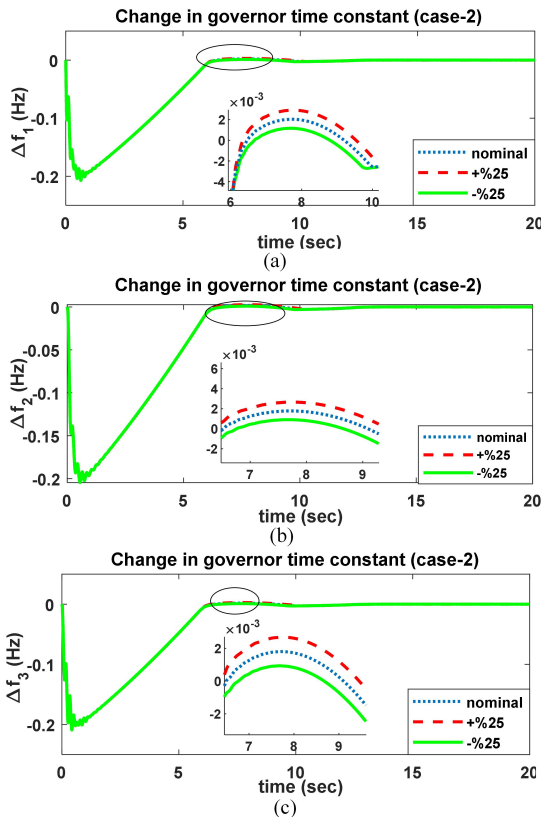


Figure 22: Response of three area system for case-3

Figure 21: Response of three area system for case-2 power systems using robust fractional pidk controller. *Ain Shams Eng J*, **9**, pp. 77–88.

Alam, M. N. (2016). Particle swarm optimization: Al-

gorithm and its codes in matlab. *ResearchGate*, **8**(1), pp. 10.Ali, E. and Abd-Elazim, S. (2013). Bfoa based design of pid controller for two area load frequency control with nonlinearities. *International Journal of Electrical Power & Energy Systems*, **51**, pp. 224–231.Arya, Y. (2018). Automatic generation control of two-area electrical power systems via optimal fuzzy classical controller. *Journal of the Franklin Institute*, **355**(5), pp. 2662–2688.Dash, P., Saikia, L. C., and Sinha, N. (2015). Automatic generation control of multi area thermal system using bat algorithm optimized pd–pid cascade controller. *International Journal of Electrical Power & Energy Systems*, **68**, pp. 364–372.Dhillon, S. S., Lather, J. S., and Marwaha, S. (2015). Multi area load frequency control using particle swarm optimization and fuzzy rules. *Procedia Computer Science*, **57**, pp. 460–472.Elgerd, O. I. and Fosha, C. E. (1970). Optimum megawatt-frequency control of multiarea electric energy systems. *IEEE transactions on power apparatus and systems*, pp. 556–563.Elsisi, M., Aboelela, M., Soliman, M., and Mansour, W. (2015). Model predictive control of two-area load frequency control based imperialist competitive algorithm. *TELKOMNIKA Indonesian Journal of Electrical Engineering*, **16**(1), pp. 75–82.Fathy, A. and Kassem, A. M. (2019). Antlion optimizer-ansf load frequency control for multi-interconnected plants comprising photovoltaic and wind turbine. *ISA transactions*, **87**, pp. 282–296.Furtat, I., Tergoev, N., Tomchina, O., Kazi, F., and Singh, N. (2016). Speed-gradient-based control of power network: Case study. *Cybernetics and Physics*, **5**(3), pp. 85–90.Guha, D., Roy, P. K., and Banerjee, S. (2018). Application of backtracking search algorithm in load frequency control of multi-area interconnected power system. *Ain Shams Engineering Journal*, **9**(2), pp. 257–276.Guo, J. (2019). Application of full order sliding mode control based on different areas power system with load frequency control. *ISA transactions*, **92**, pp. 23–34.

Gupta, M., Srivastava, S., and Gupta, J. (2013). A novel control scheme for load frequency control.

Ismail, M. M. and Bendary, A. F. (2018). Load frequency control for multi area smart grid based on advanced control techniques. *Alexandria Engineering Journal*, **57**(4), pp. 4021–4032.Ismayil, C., Sreerama, K. R., and Sindhu, T. (2014). Automatic generation control of single area thermal power system with fractional order pid ($\pi\lambda d\mu$) controllers. *IFAC Proceedings Volumes*, **47**(1), pp. 552–557.

Jagatheesan, K., Anand, B., Samanta, S., Dey, N.,

- Ashour, A. S., and Balas, V. E. (2017). Design of a proportional-integral-derivative controller for an automatic generation control of multi-area power thermal systems using firefly algorithm. *IEEE/CAA Journal of Automatica Sinica*, **6**(2), pp. 503–515.
- Lai, B. H., Tran, A.-T., Pham, N. T., and Van Huynh, V. (2021). Sliding mode load frequency regulator for different-area power systems with communication delays. *Journal of Advanced Engineering and Computation*, **5**(2), pp. 93–107.
- Mirjalili, S. (2016). Sca: A sine cosine algorithm for solving optimization problems.” a school of information and communication technology. *Griffith University, Nathan Campus, Brisbane, QLD*, **4111**.
- Morsali, J., Zare, K., and Hagh, M. T. (2017). Applying fractional order pid to design tcsc-based damping controller in coordination with automatic generation control of interconnected multi-source power system. *Engineering Science and Technology, an International Journal*, **20**(1), pp. 1–17.
- Nadimi-Shahraki, M. H., Taghian, S., and Mirjalili, S. (2021). An improved grey wolf optimizer for solving engineering problems. *Expert Systems with Applications*, **166**, pp. 113917.
- Naidu, K., Mokhlis, H., and Bakar, A. A. (2014). Multiobjective optimization using weighted sum artificial bee colony algorithm for load frequency control. *International Journal of Electrical Power & Energy Systems*, **55**, pp. 657–667.
- Padhan, D. G. and Majhi, S. (2013). A new control scheme for pid load frequency controller of single-area and multi-area power systems. *ISA transactions*, **52**(2), pp. 242–251.
- Sahu, P. C., Mishra, S., Prusty, R. C., and Panda, S. (2018). Improved-salp swarm optimized type-ii fuzzy controller in load frequency control of multi area islanded ac microgrid. *Sustainable Energy, Grids and Networks*, **16**, pp. 380–392.
- Sahu, R. K., Gorripotu, T. S., and Panda, S. (2016a). Automatic generation control of multi-area power systems with diverse energy sources using teaching learning based optimization algorithm. *Engineering Science and Technology, an International Journal*, **19**(1), pp. 113–134.
- Sahu, R. K., Panda, S., Biswal, A., and Sekhar, G. C. (2016b). Design and analysis of tilt integral derivative controller with filter for load frequency control of multi-area interconnected power systems. *ISA transactions*, **61**, pp. 251–264.
- Saikia, L. C. and Sinha, N. (2016). Automatic generation control of a multi-area system using ant lion optimizer algorithm based pid plus second order derivative controller. *International Journal of Electrical Power & Energy Systems*, **80**, pp. 52–63.
- Saini, N. and Ohri, J. (2022). Load frequency control of multi-area thermal power system using grey wolf optimization. In *Control and Measurement Applications for Smart Grid: Select Proceedings of SGESC 2021*, pp. 347–357. Springer.
- Saini, N. and Ohri, J. (2023). Optimal load frequency control of a multi-area power system with dead band effect and generation rate constraints. *Majlesi Journal of Electrical Engineering*, **17**(1), pp. 81–96.
- Sharma, Y. and Saikia, L. C. (2015). Automatic generation control of a multi-area st-thermal power system using grey wolf optimizer algorithm based classical controllers. *International Journal of Electrical Power & Energy Systems*, **73**, pp. 853–862.
- Wood, A. J., Wollenberg, B. F., and Sheblé, G. B. (2013). *Power generation, operation, and control*. John Wiley & Sons.
- Yang, J., Sun, X., Liao, K., He, Z., and Cai, L. (2019). Model predictive control-based load frequency control for power systems with wind-turbine generators. *IET renewable power generation*, **13**(15), pp. 2871–2879.